Nonstatistical fluctuations for deep inelastic processes in ^{27}Al+^{27}Al collisions

I. Berceanu,[1] M. Duma,[1] D. Moisă,[1] M. Petrovici,[1] A. Pop,[1] V. Simion,[1] A. Del Zoppo,[2] G. d'Erasmo,[3,4] G. Immé,[5] G. Lanzanò,[5] A. Pagano,[5] A. Pantaleo,[3] and G. Raciti[2,6]

[1]*National Institute of Physics and Nuclear Engineering, P.O. Box MG-6, H-76900 Bucharest, Romania*
[2]*Istituto Nazionale di Fisica Nucleare, Laboratorio Nazionale del Sud, v. S. Sofia 44, I-95100, Catania, Italy*
[3]*Istituto Nazionale di Fisica Nucleare, Sezione di Bari, v. Amendola 173, I-70126 Bari, Italy*
[4]*Dipartimento di Fisica, Universita di Bari, V. Amendola 173, I-70126, Bari, Italy*
[5]*Istituto Nazionale di Fisica Nucleare and Dipartimento di Fisica, I-95129 Catania, Italy*
[6]*Dipartimento di Fisica, Universita di Catania, I-95129 Catania, Italy*

(Received 4 January 2005; revised manuscript received 8 June 2006; published 11 August 2006)

The excitation functions (EFs) for different fragments produced in the ^{27}Al+^{27}Al dissipative collisions have been measured in steps of 250 keV in the incident energy range 122–132 MeV. Deep inelastic processes have been selected by integrating events on a total kinetic energy loss window of 12 MeV between 20 and 32 MeV. Large fluctuations are observed in all the studied EFs. Large-channel cross-correlation coefficients confirm the nonstatistical origin of these fluctuations. The energy autocorrelation function (EAF) shows damped oscillation structure as expected when a dinuclear system with a lifetime [$\tau = (5.1 \pm 2.1) \cdot 10^{-21}$s], similar with its revolution period ($T = 4.9 \cdot 10^{-21}$sec), is formed. From the periodicity of the EAF oscillations, information on the deformation of the ^{27}Al+^{27}Al dinucleus is inferred.

DOI: 10.1103/PhysRevC.74.024601 PACS number(s): 25.70.Lm, 24.60.Ky

I. INTRODUCTION

Since the experimental evidence of non-statistical fluctuations in the energy dependence of the cross section of deep inelastic processes [1], the excitation function (EF) statistical analysis became a method to obtain information on the lifetime of dinuclear systems (DNS). Naturally the question if the lifetime extracted from the EF analysis is identifiable with the value extracted previously from the angular distributions of the final fragments was addressed. The authors of Ref. [2] pointed out that the DNS lifetimes extracted by these two methods are consistent with each other. They reached this conclusion based on a reaction model in which the partial coherence, already addressed in Refs. [3,4] in connection with the degree of focusing of the angular distribution, has been considered. It was shown that the DNS lifetime extracted from the correlation width of fluctuations is assessed by the number of the partial interfering waves as is the pattern of the angular distribution. The analysis within this model has been done for the ^{28}Si+^{64}Ni [1] and ^{12}C+^{24}Mg [5] systems for which experimental information was available at that time.

Despite the expectation that the contribution of a large number of microchannels to the measured cross section should attenuate the fluctuation amplitude in the EF of the dissipative heavy-ion collisions (DHIC), the fluctuations have been observed and analyzed in EFs for other light- and medium-mass systems: ^{19}F+^{89}Y [6], ^{28}Si+^{48}Ti [7,8], ^{19}F+^{63}Cu [9], ^{28}Si+^{28}Si [10], ^{19}F+^{51}V [11]. An explanation of the persistence of the fluctuations in the EFs of DHIC is given in the framework of the partial overlapping molecular level model (POMLM) introducing, in addition to the partial coherence, the hypothesis that the DNS is excited in the low-density region of molecular levels [12,13]. The hypothesis is based on the observation that, at the measured incident energies, the intrinsic excitation energy of the composite system is a few tens of MeV above the yrast line where the level density is still expected to be low. The POMLM succeeds to describe the main characteristics of the fluctuation phenomenon in DHIC but has no predictive power. This is in contrast with the orbiting-cluster model (OCM) and the number of open channels (NOC) model [14] used for the description of the resonances in heavy-ion reactions at lower incident energies. Both models related to the concept of the "molecular resonance window" predict, with few exceptions, that the fluctuations are more intense in EFs of the reactions in which light α-nuclei are involved. The predictions of the OCM were extended to almost symmetric heavier systems such as ^{58}Ni+^{58}Ni and ^{58}Ni+^{62}Ni. These predictions were in general confirmed by the experiments at low incident energies [15,16]. In the case of DHIC one remarks that, except light systems, the nonstatistical fluctuations were observed in quite asymmetric non-α medium systems.

In this context we considered the measurement and analysis of the excitation functions for the light systems ^{19}F+^{27}Al and ^{27}Al+^{27}Al where none of the participants to the reaction are an α-conjugate nucleus to be of great interest.

For ^{19}F+^{27}Al the excitation functions have been obtained for the final fragments with $Z = 6$–12 for two total kinetic energy loss (TKEL) windows of 5 MeV width centered at 20 and 30 MeV to study the dependence of this phenomenon on TKEL. Nonstatistical fluctuations have been evidenced in the cross section EFs of the final fragments. Within the error limit no dependence on Z, TKEL, and fragment emission angle, $\vartheta_{\mathrm{c.m.}}$, has been observed for the corresponding fluctuation correlation widths, Γ [17]. An average value of Γ of (170 $\pm$ 65) keV has been obtained. The corresponding DNS lifetime $(3.9 \pm 1.1) \times 10^{-21}$ s is in agreement with the values extracted from angular distribution studies [18].

Results obtained for the ^{27}Al+^{27}Al collision are reported in the present article. After a short review of the experimental procedures and the criteria used to select deep inelastic events in Sec. II, results obtained from cross-section EFs analysis for the ^{27}Al+^{27}Al system are reported in Sec. III A. The influence of the evaporation corrections on the fluctuating structure of EF is presented in Sec. III B. A pattern of the energy autocorrelation function with secondary damped oscillations in addition to the Lorentzian structure from $\varepsilon = 0$, where ε is the energy increment in the center-of-mass (c.m.) system, was obtained. The observed periodicity of the oscillation could be explained if deformed rotational states are supposed to be excited in DNS during the collision [19,20]. This aspect is discussed in Sec. III C. Conclusions are presented in Sec. IV.

II. EXPERIMENTAL PROCEDURES

The experiment was performed at the SMP Tandem accelerator from LNS-Catania using ^{27}Al ions with incident energies $E_{\rm lab} = (122–132)$ MeV. The energy loss in self-supported targets of ^{27}Al (≈75 keV) is less than the energy increment of 250 keV (125 keV in the c.m. system) between two successive experimental points. The beam current was measured with a tantalum-plated Faraday cup provided with an electron suppressing guard ring. To minimize the carbon contamination the target was changed two times during the experiment. The estimation of this contamination is based on measurements at $E_{\rm lab} = 121.5$ and 127.25 MeV in which a carbon target with thickness of 100 μg/cm^2 was used.

The reaction products were detected and identified using the experimental device DRACULA [18] from which only the large area position sensitive ionization chambers (ICs) and the corresponding parallel plate avalanche counters in front of them have been operated. The ICs were filled with Ar(90%)+CH_4(10%) at 106.8 torr. The polar and azimuthal angles spanned by the IC were $\Delta\vartheta = 24^\circ$, $\Delta\varphi = 4^\circ$, respectively. The energy resolution at the elastic peak was 2.5%, the angular resolution 0.5° and the charge resolution better than 0.3 charge units. The ICs being centered at 24° in the laboratory system, an angular range $12^\circ \leqslant \vartheta_{\rm lab} \leqslant 36^\circ$ was covered continuously in a single measurement for each incident energy. The grazing angle at $E_{\rm lab} = 132$ MeV is of ≈15°, so the weight of deep inelastic processes was increased within the measured angular interval. Nevertheless, a quasielastic component is present in the TKE spectra of fragments with $Z = 11$, 12 as can be seen in Fig. 1 for $E_{\rm lab} = 128$ MeV. The arrows on the panels of Fig. 1 indicate the energy of totally relaxed events for corresponding final fragmentations calculated with the formula for asymmetric fission [21], $\mathrm{TKE}^{af} = \mathrm{TKE}^{f} Z_P Z_T/(Z_C^2/2)$, where Z_P, Z_T, and Z_C are the atomic numbers for projectile, target, and composite systems, respectively. The most probable TKE value released in fission, TKE^{f}, was calculated with the formula from Ref. [22].

The excitation functions for deep inelastic processes are obtained taking events with TKE larger than TKE^{af} values and well below the quasielastic component. The TKE window used for $E_{\rm lab} = 128$ MeV is represented by the hatched area on Fig. 1 and corresponds to the total kinetic energy loss window from 20 to 32 MeV, kept the same for all incident energies.

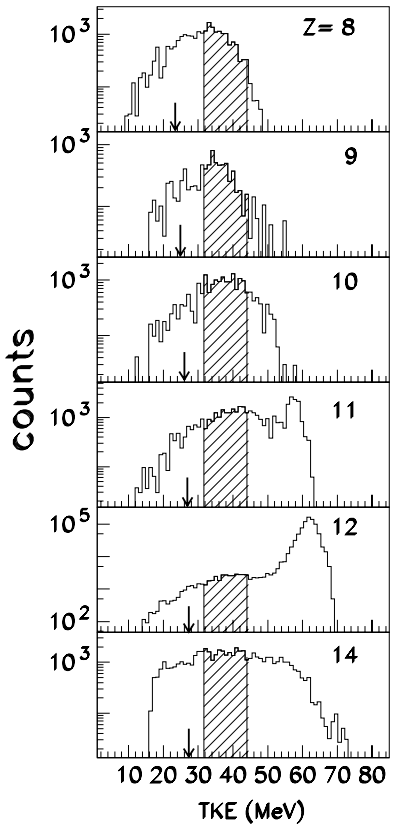

FIG. 1. Total kinetic energy spectra for $Z = 8$–12, 14 reaction products in the ^{27}Al+^{27}Al collision at incident energy $E_{\rm lab} =$ 128 MeV. The arrows indicate TKEs of totally relaxed events for corresponding fragmentations calculated as it is described in text.

As it was mentioned above, to reduce the carbon contamination, the target was changed two times during the experiment. For the evaluation of carbon contamination, the measurements before and after the target change and those on the carbon target have been used. The contribution of the processes on the carbon impurities to the yield of the fragments with $Z \neq 13$ in the considered TKEL window was found to be negligible. This result was obtained using the charge distribution and the angular distribution of $Z = 13$ fragments from ^{27}Al+^{27}Al and ^{27}Al+^{12}C interactions at $E_{\rm lab} = 121.5$ and 127.25 MeV. From the charge distribution (normalized to the beam current) the fragment yields in the considered TKEL window (Table I) have been obtained for Al projectiles incident on 40 μg/cm^2 Al (thickness of the used targets) and 100 μg/cm^2 C. One has to remark the much lower yields of the fragments with $Z \neq 13$ in the ^{27}Al+^{12}C interaction. This is because of the fact that the selection of events with TKEL = (20–32) MeV from the interaction ^{27}Al+^{27}Al means, for example, a TKE = (28.75–40.75) MeV at $E_{\rm lab} =$ 121.5 MeV and events with such values of TKE because of carbon contaminant are of quasielastic origin ($E_{\rm c.m.}^{\rm max} =$

TABLE I. Fragment yields in a TKEL = (20–32) MeV window for ^{27}Al projectiles incident on the ^{27}Al (40 μg/cm^2) and carbon (100 μg/cm^2) targets.

Z	6	7	8	9	10	11	12	13	14
^{27}Al+^{27}Al, 121.5 MeV	0.022	0.053	0.206	0.073	0.213	0.268	0.630	0.827	0.271
^{27}Al+^{12}C, 121.5 MeV	0.006	0.019	0.036	0.009	0.008	0.056	0.096	3.358	0.040
^{27}Al+^{27}Al, 127.25 MeV	0	0.031	0.204	0.096	0.265	0.370	0.706	0.828	0.374
^{27}Al+^{12}C, 127.25 MeV	0	0.005	0.005	0.005	0.009	0.034	0.069	1.521	0.018

33.4 MeV of ^{27}Al scattered on carbon at 12.5°). The difference found in the yields (normalized to the beam current) for $Z = 13$ fragments before and after the change of the target at both energies ($E_{\rm lab} = 125.5$ and 131.5 MeV) was of ∼0.09, which should correspond to a carbon deposition of 6 μg/cm^2 if one considers the yield on the carbon target at $E_{\rm lab} =$ 127.25 MeV. The effect of such a deposition on the yield of fragments with $Z \neq 13$ is $\leqslant$1%. Indeed, for these fragments we observed no difference in the error limits in the yields before and after the change of the target.

We also did an estimation of the effect of carbon contamination using angular distributions. Figures 2(a) and 2(c) show the angular distributions (normalized to the beam current) for $Z = 13$ fragments with TKEL = (20–32) MeV produced by ^{27}Al projectiles incident on Al target (full line) and 10 μg/cm^2 C (dashed line) at $E_{\rm lab} = 121.5$, 127.25 MeV, respectively. In the right-panels one can see what should be the effect on the angular distribution of fragments with $Z = 13$ corresponding to a 10 μg/cm^2 C deposition on Al target (full line). The dashed line is the angular distribution of events from an Al target without carbon deposition. For $E_{\rm lab} = 121.5$ MeV a second peak at $\vartheta \approx 42°$ should evidence in the angular distribution, whereas at $E_{\rm lab} = 127.25$ MeV because of a lower yield of $Z = 13$ fragments it should manifest for a 15 μg/cm^2 C deposition. For the last case the contributions of carbon impurities to $Z \neq 13$ events should be of ≈2%. In fact we did observed no two-peaked angular distribution at any energy. This confirms the previous result that the deposition before the change of the target is less than 10 μg/cm^2 C.

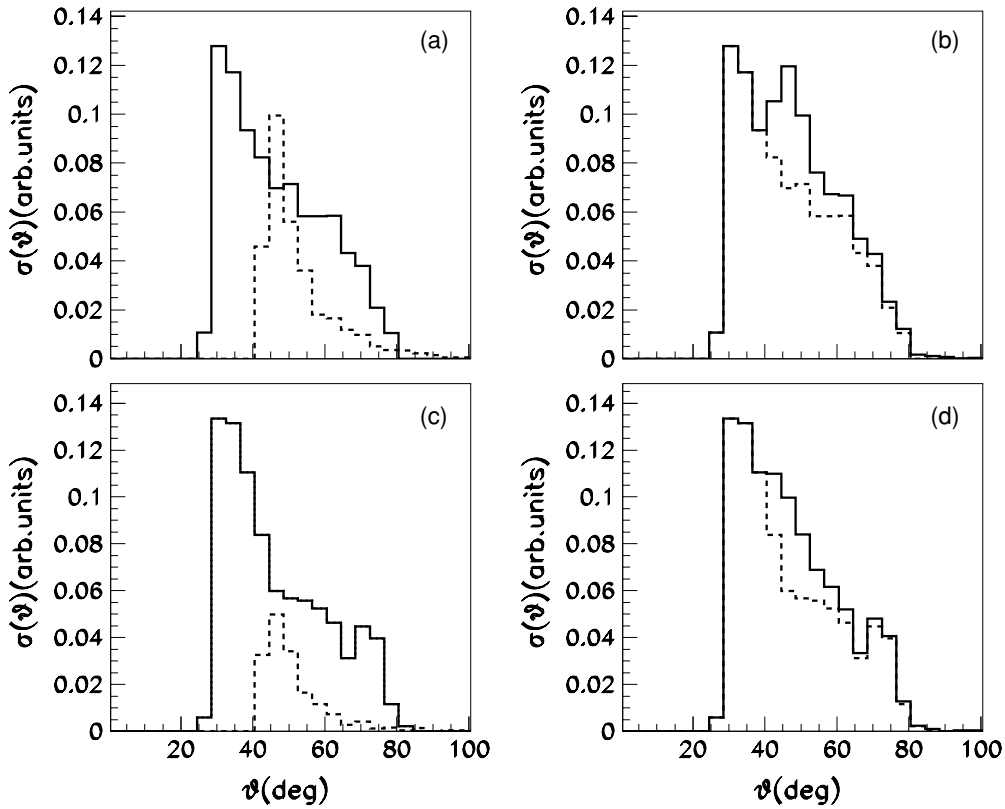

FIG. 2. Angular distribution (normalized to the beam current) of $Z = 13$ fragments with TKEL = (20–30) MeV produced by (a) and (c) ^{27}Al target (40 μg/cm^2) (full line) and 10 μg/cm^2 ^{12}C (dashed line); (b) and (d) Al target with 10 μg/cm^2 C deposition (full line) and Al target without carbon deposition (dashed line) at $E_{\rm lab} = 121.5$, 127.25, respectively.

III. CROSS SECTION EXCITATION FUNCTIONS

A. Statistical analysis

1. Energy autocorrelation function: experimental results and discussion

The obtained excitation functions corresponding to $Z =$ 8–12, 14 are represented in Figs. 3(a)–3(e). The full circles represent the cross section of the primary products and the empty triangles of the secondary ones.

The influence of the evaporation corrections on the EFs, obtained by comparing the results for these two sets of EFs, are discussed in Sec. III B. In the following we refer only to the analysis of the EFs for primary products. Fluctuations with amplitudes larger than the statistical errors, which are of point size, could be observed. The statistical analysis of the EFs has been done following the recipe from Ref. [23]. The fluctuations from the EFs corresponding to different final channels are strongly correlated, evidenced by large-channel cross-correlation coefficients, $C_{Z_i Z_j}$, presented in Table II. This shows that the observed fluctuations are not of compound

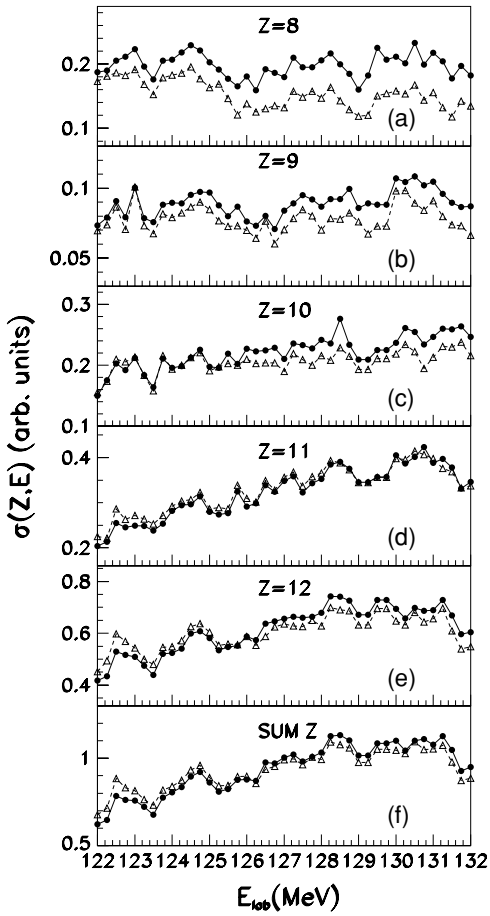

FIG. 3. Excitation functions for $Z = 8$–12 fragments with TKEL = (20–32) MeV produced in the ^{27}Al+^{27}Al reaction [panels (a)–(e)], and summed EF of $Z = 11$ and 12 products [panel (f)]; the full circles represent the EFs after evaporation corrections (for primary products) and the empty triangles the EFs without evaporation corrections (for secondary products).

TABLE II. Channel cross-correlation coefficients $C_{Z_i Z_j}$.

Z	8	9	10	11	12
8	1	0.865	0.702	0.356	0.467
9		1	0.482	0.671	0.554
10			1	0.831	0.977
11				1	0.703
12					1

nucleus origin. Taking into account this correlation, to improve the statistics, an EF was obtained by summing the EFs for reaction products with the atomic number close to Z of the projectile ($Z = 11$ and 12), which is given in the bottom panel of Fig. 3.

The energy autocorrelation function has been calculated with [23]:

$$C(\varepsilon) = \left\langle \left[\frac{\sigma(Z,E)}{\overline{\sigma}(Z,E)} - 1 \right] \left[\frac{\sigma(Z,E+\varepsilon)}{\overline{\sigma}(Z,E+\varepsilon)} - 1 \right] \right\rangle,$$

where ε is the energy increment in c.m. system and $\overline{\sigma}(Z,E)$ represents the energy averaged cross section. The experimental energy autocorrelation functions for the reaction products with $Z = 8$, 12 and for the summed EF are shown in Fig. 4 with full circles. The average of the cross section over the incident energy has been obtained using the moving Gauss averaging procedure [24]. In addition to the structure from $\varepsilon = 0$, supplementary oscillations specific to EAF of the excitation function in case of deep inelastic processes are present. One has to remark also that the supplementary structure is quite different for the reaction products with Z close ($Z = 12$) to and far ($Z = 8$) from the projectile one. This aspect and the information obtained from the supplementary structure is discussed in Sec. III C. The fluctuation correlation widths Γ_p, extracted by fitting the experimental EAFs with a Lorentzian function (thick dashed line in the same figure), are given in the first column of Table III. The error of ≈25% in the evaluation of Γ_p is mainly because of the finite range of data (FRD). As in the case of the ^{19}F+^{27}Al system no dependence of the correlation width on the atomic number is observed. At a value of $\Gamma_p = (128 \pm 32)$ keV obtained for the summed EF corresponds a lifetime of $(5.1 \pm 2.1) \times 10^{-21}$ s for the ^{27}Al+^{27}Al DNS, specific to a DNS formed in the first stage of a heavy-ion interaction.

The correlation width obtained by us is within the error limit in agreement with the value of $\Gamma = (150 \pm 75)$ keV obtained from the analysis of the EF for dissipative collisions in the

TABLE III. Energy correlation widths Γ_p and Γ_s for primary and secondary products, respectively.

Z	Γ_p(keV)	Γ_s(keV)
8	100 ± 25	113 ± 29
11	115 ± 29	122 ± 31
12	104 ± 26	115 ± 29
Sum Z	128 ± 32	120 ± 30

^{27}Al+^{27}Al system analyzed in a lower incident energy interval ($E_{\text{c.m.}} = 58$–60.9 MeV) in Ref. [13]. As it was mentioned above the error on the Γ value is mainly because of FRD error, which is $\sim(n)^{1/2}$, where n is the number of the uncorrelated experimental points. A reduction factor in errors because of the FRD of ≈1.7 is obtained in the present data relative to Ref. [13].

The Γ value obtained in the present analysis and the one previously published for ^{19}F+^{27}Al are much larger than those estimated with the empirical formula [25]:

$$\Gamma_{\text{CN}} = 14 \exp\left(-4.69\sqrt{\frac{A_{\text{CN}}}{E^{\star\text{ef}}_{\text{CN}}}}\right) \text{MeV}, \qquad (1)$$

which describes the systematics of the average compound nucleus decay widths for light nuclei [26]. In formula (1) A_{CN} and $E^{\star\text{ef}}_{\text{CN}}$ are the mass number and intrinsic excitation energy of the composite system. The intrinsic excitation energy per nucleon available in the ^{27}Al+^{27}Al and ^{19}F+^{27}Al systems can be seen in Fig. 5.

The continuous line represents, as a function of the angular momentum, the barrier energy $E_B = V_{\text{CB}} + E_{\text{rot}}$, where

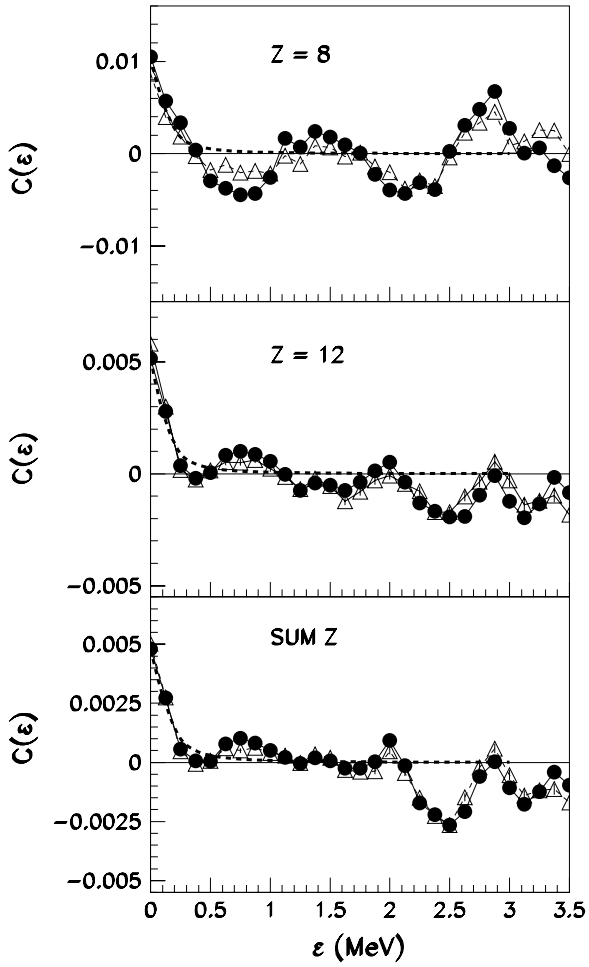

FIG. 4. Experimental energy autocorrelation functions (points) and the fit with a Lorentzian function (dashed line); the full circles represent the EAF for primary products and the empty triangles for secondary ones.

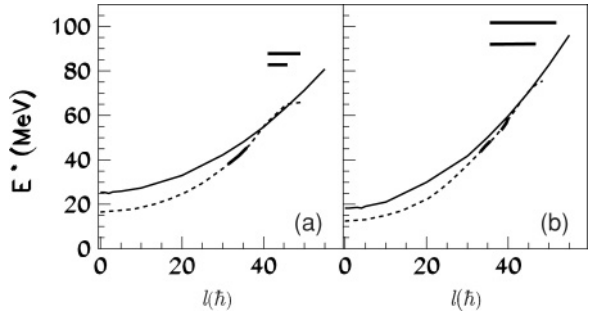

FIG. 5. Excitation energy for (a) ^{27}Al+^{27}Al system and (b) ^{19}F+^{27}Al system; the horizontal lines delimit the entry region on the available l window corresponding to the lower and upper limit of the incident energy; the continuous line represents the barrier energy, the dashed line TKEL as a function of l calculated with the DONA code, the thick zones on this line correspond to the considered TKEL windows.

V_{CB} is the Coulomb barrier and E_{rot} is the energy of the rotational level sequence. The horizontal lines correspond to the excitation energies of the ^{54}Fe and ^{46}Ti compound nuclei for the lower and upper limit of the incident energy and the available l window. The centroid of the l window corresponds to the intrinsic excitation energy $E^{\star\text{ef}}_{\text{CN}} = E^{\star}_{\text{CN}}$-$E_B \approx$ 27 (32) MeV in ^{54}Fe (^{46}Ti) CN for the upper incident energy ($E_{\text{lab}} = 132$ MeV). A width of ≈12 (60) keV for excited levels in ^{54}Fe (^{46}Ti) CN is estimated using the semiempirical formula given by Eq. (1).

The values of the coherence widths obtained in the present work and those of Refs. [6,8–11,13,17] as a function of $\sqrt{A_{\text{CN}}/E^{\star\text{ef}}_{\text{CN}}}$ are represented in Fig. 6. We included in this representation only the Γ values extracted by the EAF method. The full (empty) circles represent Γ values for light (medium) systems. The line represents the Γ_{CN} systematics for light nuclei [Eq. (1)]. One can see that the Γ values of the fluctuations from the EFs of DHIC are rather independent of the parameter $\sqrt{A_{\text{CN}}/E^{\star\text{ef}}_{\text{CN}}}$. A tendency of separation between light and medium systems could be observed, but the data are too scarce to draw a definite conclusion. A similar behavior was observed to be characteristic to intermediate structures at lower incident energies as well [15].

2. *Angular analysis: experimental results and discussion*

The time scale of the reaction could also be estimated by the Regge pole analysis of the angular distributions. In Figs. 7(a) and 7(b) are represented the average angular distributions for $Z = 8$ fragments and the sum of the $Z = 11$ and 12 products, respectively. The angular distribution for the fragment with atomic number away from the projectile one is flat showing the increase of the degree of inelasticity of the reaction with increasing number of transferred nucleons, whereas that of $Z = 11 + 12$ products is specific for faster processes. Nevertheless in the last case one can observe a change of the slope of the angular distribution around 50° which can be assigned to the increase of the contribution of slower processes to these fragmentations at backward angles.

The dashed lines in Fig. 7 are obtained with Regge pole model analysis [27]. The corresponding lifetime of DNS is 1.8×10^{-21} s, 7.2×10^{-22} s for $Z = 8$, $11 + 12$ products, respectively. Similar DNS lifetimes have been obtained for this system from the angular distribution measured on a larger angular range at a fixed energy, $E_{\rm lab} = 140.14$ MeV [28]. We also fitted separately the forward and backward part of the average angular distribution for the $Z = 11 + 12$ products obtaining for the DNS lifetime a value of 5.5×10^{-22} s and 1.4×10^{-21} s, respectively. This shows that for the present data (present energy increment between two consecutive measurement points), the DNS lifetime extracted by fitting the Lorentzian part of the EAF seems consistent with the lifetime extracted from the angular distribution corresponding to slower processes that take place during the reaction. The faster processes manifest in supplementary structure of the EAF similar with the long-range oscillation because of the rotation of the DNS. We could not determine the width of this structure by the EAF method from the dependence of $C(0)$ on the averaging interval, as described in the Ref [24], where only one plateau was reached. The way of estimation of the long-range oscillation related to the DNS rotation is discussed in Sec. III C.

The study of the EF is also used to obtain information concerning the level density. This possibility was already evidenced in connection with Ericson fluctuations [29]. For DHIC a relationship between $V = [C(0)]^{1/2}$ and the level density in the framework of POMLM [13] was obtained:

$$V = 1.5(\Delta)^{-\frac{1}{1+\gamma}} \frac{\sigma_S}{\sigma_F + \sigma_S} \sqrt{\frac{D}{\Gamma}}, \qquad (2)$$

where Δ is the angular momentum window, $\gamma = \Gamma/\hbar\omega$ gives the degree of the angular momentum coherence and σ_S, σ_F are the cross sections for slow and fast processes, respectively.

The level density for the systems ^{28}Si+^{28}Si and ^{27}Al+^{27}Al was obtained in Refs. [10,13] using Eq. (2). In the following we also make an evaluation of the level density using this method.

Figure 8 shows (full circles) the square root of the normalized variance V as a function of $\vartheta_{\rm c.m.}$ extracted from EAFs of the excitation functions corresponding to the sum on Z by integrating on the angular range of $\Delta\vartheta_{\rm c.m.} = 4^\circ$ and the same TKEL window (20–32 MeV). The obtained pattern of V as a function of $\vartheta_{\rm c.m.}$ is quite similar with that from Ref. [13] (full squares in Fig. 8) but in our case the values of V are larger by a factor of ≈3. The difference could be explained by the fact that the integrating TKEL window is narrower with 8 MeV and the analysis is done on a larger incident energy interval than that in Ref. [13]. To study the influence of the energy interval range on the V values we calculated the square root of the normalized variance as a function of $\vartheta_{\rm c.m.}$ corresponding to the subintervals equal to the energy interval used in Ref. [13] (3 MeV in the c.m. system). The result for one of the subintervals, that beginning with $E_{\rm lab} = 125$ MeV, is presented in Fig. 8 with empty circles. One can see a decrease of V when it is calculated using a smaller incident energy interval mainly because of FRD errors. At the end of this subsection a discussion on the influence of the integrating window on the C(0) (V) values is given.

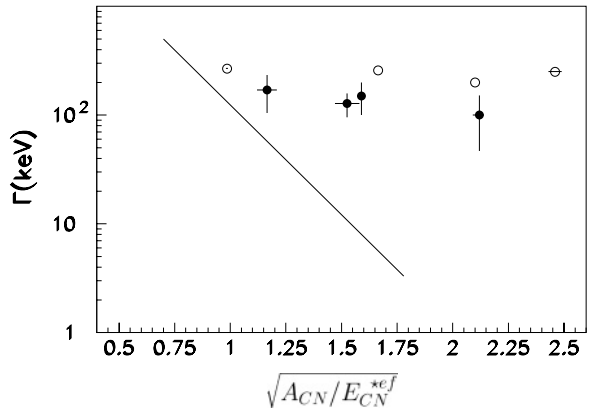

FIG. 6. Γ values of the fluctuations from the EFs for dissipative processes in ^{19}F+^{27}Al [17], present article, ^{27}Al+^{27}Al [13], ^{28}Si+^{28}Si [10] (full circles from the left to the right), ^{19}F+^{63}Cu [8], ^{19}F+^{51}V [11], ^{19}F+^{89}Y [6], and ^{28}Si+^{48}Ti [9] (empty circles from the left to the right) as a function of $\sqrt{A_{\rm CN}/E^{*\rm ef}_{\rm CN}}$. The thin line represents the compound nucleus $\Gamma_{\rm CN}$ values [Eq. (1)].

Using the above formula the authors of Ref. [13] obtained $\Gamma/D = 13$ with a quite large uncertainty, 10–40, because of errors with which the parameters from Eq. (2) were determined. For such a value of Γ/D, when only a partial overlapping of the DNS levels takes place, it was shown that in the simulated excitation functions still persist significant fluctuations [12,13].

The value of Δ depends on the reaction mechanism and for deep inelastic processes it is of the order of $\Delta \approx ka$ [3], where k is the asymptotic wave number and a the nuclear surface diffuseness. With $\Delta \approx 3.5$, $\gamma = 0.14$ as obtained from the present data and considering a slow component of 50% a value of $\Gamma/D \sim 6$ is obtained. For a lower value of Δ, e.g., 2 as was found in Ref. [13] for slower processes, one obtains for Γ/D a value of 16. These values are within the Γ/D range estimated in Ref. [13].

For deep inelastic processes $C(0) \propto 1/N_{\rm eff}$, where $N_{\rm eff}$ is the number of effective microchannels contributing to the considered cross section [30]. In our article analyzing the excitation functions of the ^{19}F+^{27}Al system [17] an increase of $N_{\rm eff}$ was observed by increasing the integration window (TKEL, $\vartheta_{\rm c.m.}$), but not proportional with the window width, reflecting the fact that in the case of deep inelastic processes it is not so clear how to weight the independent microchannels contributing to the cross section [30]. This aspect is confirmed by the present analysis. For example, decreasing the angular range of integration from the whole available angular range ($\Delta\vartheta_{\rm c.m.} = 24^\circ$–$72^\circ$) to windows of $\Delta\vartheta_{\rm c.m.} = 4^\circ$ the $C(0)$ increases from ∼0.005 (see Fig. 4) to ∼0.01 (Fig. 8). In view of this discussion, the fact that in our case the TKEL window is narrower and we analyzed the EF summed only on $Z = 11$ and 12, whereas in Ref. [13] the summation is done from $Z = 11$ to $Z = 15$, the larger V values obtained by us even for an incident subinterval energy of 3 MeV seem quite justified.

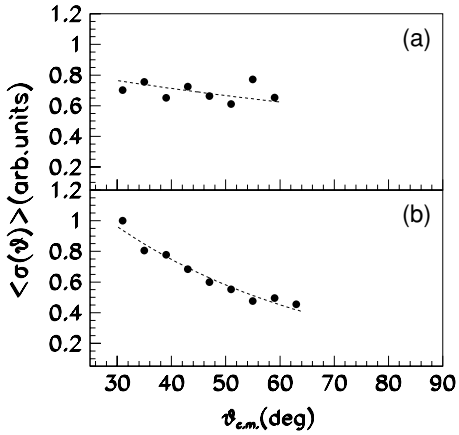

FIG. 7. Average angular distribution: the full circles represent experimental points for (a) $Z = 8$ and (b) $Z = 11 + 12$ fragments, the dashed line represents the fit obtained by the Regge pole analysis.

The low value of Γ/D obtained on the basis of the square root of the experimental variance sustains the hypothesis of the POMLM. The partial overlapping of the DNS levels together with the quite low number of effective channels that seem to contribute to the considered cross sections (∼200 for integration done on the whole available angular range and considering equally weighted microchannels contributing to the cross section) could explain the fact that the fluctuations in the excitation functions of deep inelastic reactions are not completely damped and could be observed.

B. Influence of the evaporation corrections on cross section EF

The extended theory of Ericson fluctuations [30] and the other models developed to explain the presence of nonstatistical fluctuations in DHIC are elaborated for primary reaction products. Experimentally are measured observables of the secondary products and for comparison with models, evaporation corrections have to be done. The observables of the primary products were obtained by taking into account the nucleon evaporation using the iterative procedure

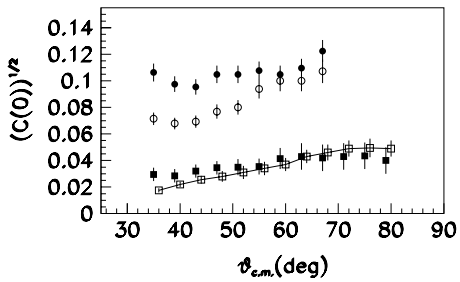

FIG. 8. Square root of the variance as a function of $\vartheta_{\text{c.m.}}$: the full circles represent the experimental points obtained in the present article using the whole incident energy interval, the empty circles those corresponding to a subinterval of 3 MeV in c.m. system (for details see the text), the full squares the experimental points from Ref. [13] and the empty squares the calculated ones in the same article using POMLM.

described in Ref. [31]. The procedure has been adapted for the investigated system as in Ref. [18]. As mentioned in Sec. III A1, the EFs of the primary reaction products are represented with full circles in Fig. 3. To estimate the influence of the evaporation corrections on the EFs, we also constructed a set of EFs for secondary products integrating on the reaction products observable values before the evaporation corrections. These are represented with empty triangles in Fig. 3. Qualitatively no sizable differences between the two sets of EFs could be seen. For a more quantitative evaluation, we calculated the energy autocorrelation functions of these EFs. They are represented with empty triangles in Fig. 4. The extracted Γ_s values for secondary products are given in the second column from Table III. One can conclude that within the error limits no modification of the oscillation structure in the EFs is observed with the evaporation correction procedure for the present data. It is not clear to which extent this conclusion could be extended to higher excitation energies.

C. Deformation of the dinuclear system

The experimental EAFs from Fig. 4 show besides the Lorentzian structure at $\varepsilon = 0$ secondary oscillations. Such pattern of EAF was observed in previous studies of EF for DHIC [6,10,13,17]. It was shown that these oscillations appear when the lifetime of DNS is equal or greater than its rotation period as a result of interference between different revolutions [32,33]. For symmetric systems [20] the period of the secondary structures is given by:

$$\varepsilon_c = 2\hbar\omega, \tag{3}$$

where $\omega = l\hbar/\mathcal{J}$ is the angular velocity of the dinucleus. The total momentum of inertia is in the sticking configuration $\mathcal{J} = \mathcal{J}_{\text{rel}} + \mathcal{J}_{\text{int}}$, where $\mathcal{J}_{\text{rel}} = 1.044\,\mu\,r^2 \times 10^{-46}\text{MeV s}^{-2}$ and $\mathcal{J}_{\text{int}} = (2/5)1.044 r_\circ^2 (A_3^{5/3} + A_4^{5/3}) \times 10^{-46}\text{MeV s}^{-2}$ [34], A_3, A_4 being the atomic masses of the fragments.

By evaluating the separation distance r between the fragments from the most probable total kinetic energy ⟨TKE⟩ one can estimate with Eq. (3) a value for ε_c that can be compared with experimental values observed in EAF.

The ⟨TKE⟩ of the fragments equals the final channel barrier [35,36]:

$$\langle \text{TKE} \rangle = 1.44 \frac{Z_3 Z_4}{r} + \frac{\hbar^2 l(l+1)}{2\mathcal{J}_{\text{rel}}}.$$

From ⟨TKE⟩ ≈ 33 MeV for $Z = 8$ (the corresponding panel of Fig. 1), one deduces a separation distance $r \approx 10.9$ fm. This evaluation is obtained for the angular momentum of the sticking configuration $l_{\text{st}} = l(1 - \mathcal{J}_{\text{int}}/\mathcal{J}_{\text{tot}})$, where $l = (l_{\text{gr}} + l_{\text{cr}})/2$. For l_{gr} we used the value of $47.8\hbar$ calculated with the DONA code for $E_{\text{lab}} = 128$ MeV and $l_{\text{cr}} = 43.7\hbar$ was calculated using the formula given in Ref. [21]. For this separation distance and $l = l_{\text{st}}$ one obtains a period of 1.7 MeV using Eq. (3). One can observe in the EAF of fragment with $Z = 8$ (Fig. 4) that large period oscillations of ≈1.5 MeV are very well evidenced.

⟨TKE⟩ ≈ 41 MeV for $Z = 12$ (Fig. 1) equals the final channel barrier for a separation distance $r \approx 10.0$ fm. For

the long-range oscillation one obtains with Eq. (3) a period of 2.0 MeV. One can see (second and third panels of Fig. 4) that there is a signal in this region of the EAFs for $Z = 12$ and $Z = 11 + 12$ but before the bump at 2 MeV there are other oscillations which diminish the visibility (the difference between the maximum and minimum) of the long-range structure. They could be because of the quite large contribution of the faster process to this fragmentation. Such oscillations are not seen in the EAF of $Z = 8$ where the slow process is dominant as shown by the angular distribution.

TKEL $= f(l)$ calculated with a transport model (DONA code) [37] for the upper limit of the measured energy interval is represented with dashed line in Fig. 5(a). The thick zone on this line corresponds to the TKEL window used in the present analysis. One has to remark that the used values for l_{st} (30.0$\hbar$ and 32.5$\hbar$ for O+Ar and Mg+Si fragmentations, respectively) lie within the l window ($l = 30$–$35\hbar$) given by the transport model calculation. This shows that the model describes quite well the dissipative processes in the light systems too, as already noticed in our first study [38].

The determined separation distance is affected mainly by the considered average angular momentum, in the evaluation of which l_{cr} has the largest uncertainty. Because of shell effects, the experimental values of l_{cr} for light heavy-ion systems in the mass region 55–60 have a large spreading (27$\hbar$–42$\hbar$) as can be seen in Table I of Ref. [39]. We preferred to consider the calculated value of this observable as in Ref. [21] to keep the same procedure as for the ^{19}F+^{27}Al system. This value is in quite good agreement with $l_{cr} = 42\hbar$ obtained from the reaction ^{28}Si+^{27}Al at $E_{lab} = 150$ MeV [40]. However, for the compound nucleus ^{56}Ni excited at 80 (90) MeV corresponding to the lower (upper) excitation energy of the composite system in the present measurement, a lower value of l_{cr} was evaluated from the sharp cutoff model, $l_{cr} = 39(41)\hbar$ [41]. The estimation of the separation distance by calculating the mean angular momentum with a lower value of l_{cr} seems justified. Applying the procedure described before using $l_{cr} = 35\hbar$ we obtained 10.3 fm (9.5 fm) for O+Ar (Mg+Si) fragmentation. The ε_c values calculated with Eq. (3) are 1.4 and 1.6 MeV for O+Ar and Mg+Si fragmentations, respectively. This shows that a lower value of l_{cr} is more appropriate to describe the long-range oscillations from $Z = 8$ EAF, whereas they are quite well reproduced with $l_{cr} = 43.7\hbar$ for the fragments with atomic number close to the projectile one.

The obtained separation distance values mean a quite large deformation for the reaction partners of the DNS. For the relative momentum of inertia at a separation distance $r =$ 10.9 fm, the following relation can be written:

$$\mathcal{J}_{rel}(r) = 1.97\mathcal{J}_{rel}(R_{int}), \tag{4}$$

where $R_{int} = r_\circ(A_3^{1/3} + A_4^{1/3})$ ($r_\circ = 1.3$) is the interaction radius for spherical interacting nuclei. The low-level density deduced for the ^{27}Al+^{27}Al DNS on the basis of Eq. (2) could have an explanation in the excitation of some special states of the (super-) deformed rotating DNS that do not mix with high-density levels of CN nature.

It was also necessary to consider larger momenta of inertia to explain the period of the secondary oscillations observed in the EAF for other systems (^{12}C+^{24}Mg, ^{24}Mg+^{24}Mg, and ^{28}Si+^{28}Si) in this mass region [19,20], whereas the period of the secondary structures in the EAF for heavier systems (^{19}F+^{89}Y [32], ^{58}Ni+^{58}Ni, ^{58}Ni+^{62}Ni [16], ^{58}Ni+^{46}Ti [42]) could be explained using the momentum of inertia calculated at R_{int}. This shows the possibility of the existence of super- and hyperdeformation in this mass region, as it was predicted 30 years ago [43]. RLDM predicts, for example, triaxial ^{54}Fe and ^{46}Ti CNs for angular momentum greater than 33.6$\hbar$ and 29$\hbar$, respectively.

The authors of Ref. [43] concluded their article as follows: "The outstanding problem is to devise methods that would identify the presence of such superdeformed nuclei which in some existing experiments have been produced without having been detected." Meanwhile, experimental methods to evidence the existence of such nuclei have been developed. One should notice results of recent experiments providing information on nuclear deformation in the mass region close to the mass of the dinuclear systems studied in the present article, which appears to be a very interesting one from this point of view.

For ^{27}Al+^{27}Al at lower incident energies [13] it is mentioned that to explain the large period of oscillation a moment of inertia increased by 30% with respect to a sticking configuration should be considered. There are many studies for systems with masses close to this value, the most intensive being related to the reaction ^{28}Si+^{28}Si.

The theoretically predicted triaxial nuclear molecule ^{28}Si+^{28}Si constructed on the ground-state oblate deformation of the ^{28}Si nucleus [44] was experimentally evidenced by the detailed study of the resonance with $J^\pi = 38^+$ in ^{56}Ni [45,46].

Light-charged-particle spectra emitted by ^{56}Ni, ^{55}Co, and ^{59}Cu compound nuclei in the reactions ^{28}Si+^{28}Si [39], ^{28}Si+^{27}Al [41] and ^{35}Cl+^{24}Mg [47] were measured and it was shown that they could be described by calculating the yrast line with an effective moment of inertia $\mathcal{J}_{eff} = \mathcal{J}_{sphere}(1 + \delta_1 l^2 + \delta_2 l^4)$, where δ_1, δ_2 are the deformability parameters and $\mathcal{J}_{sphere}$ is the rigid body moment of inertia. For deformability parameter values deduced from the fit of experimental spectra, one obtains for the effective moment of inertia $\mathcal{J}_{eff} \approx 1.5\,\mathcal{J}_{sphere}$ for the above compound nuclei. Eq. (4) obtained for the dinucleus ^{27}Al+^{27}Al is similar to this. The relative momentum of inertia at breakup obtained by us can also be seen as an effective one introduced to reproduce the experimental periodicity of the EAF.

If at present time there are not yet other experiments dedicated to the study of the deformation of the dinucleus ^{27}Al+^{27}Al, the CN ^{46}Ti corresponding to the dinucleus ^{19}F+^{27}Al, for which we also found a large separation distance ($r \approx 11$ fm), became in the last period subject of intensive studies [48–50]. In this mass region the α-particle spectra emitted in the reaction ^{16}O+^{28}Si [51] were studied initially. The set of deformability parameters δ_1 and δ_2 describing the α spectral shape at three incident energies indicate a large deformation of the ^{44}Ti CN (axis ratio $a/b \approx 2$). More recently [48] the Lublin-Strasbourg Drop model has been used to calculate Jacobi transition mechanism in ^{46}Ti [48]. The γ-ray spectrum from the decay of GDR built in hot ^{46}Ti produced in the collision ^{18}O(105 MeV)+^{28}Si was measured and its shape could be described supposing an elongated three-axial equilibrium shape for this nucleus at $l = 30\hbar$

[48,49]. The description of α-particle spectra emitted by the compound nucleus ^{46}Ti populated in the reaction ^{27}Al+^{19}F suggests also the occurrence of very elongated shapes around this value of the angular momentum [50]. The excitation functions for the system ^{19}F+^{27}Al (dinucleus ^{46}Ti) have been constructed for TKEL windows centered at 20 and 30 MeV [thick zones on the dashed line from Fig. 5(b)]. One can see that for these TKEL windows correspond angular momentum values near the region where very elongated shapes could appear.

The results obtained in the present article and in the previous ones [17,19,20] on the basis of long-range oscillations in the EAF evidence a large deformation of the composite systems formed in the first stage of elastic, inelastic scattering, and deep inelastic processes in the mass region 36–56. Thus, one can consider the analysis of the cross section EFs as an experimental method to evidence and extract information on such elongated objects.

IV. CONCLUSIONS

Large fluctuations have been evidenced in the EF for deep inelastic processes in the ^{27}Al+^{27}Al interaction on the incident energy interval (122–132) MeV. The large-channel cross-correlation coefficients and the EAF pattern different from a Lorentzian shape show the nonstatistical origin of the fluctuations. The correlation width of the fluctuations extracted from the cross-section EF is equal to (128 ± 32) keV to which corresponds a DNS lifetime of $(5.1 \pm 2.1) \times 10^{-21}$ s. This lifetime is in good agreement with the DNS lifetime extracted from the average angular distribution. The low value for Γ/D estimated in the POMLM framework is physically supported by the excitation of the deformed DNS levels in a region at $\sim$27 MeV above the yrast line. Similar characteristics have been found previously for the fluctuation phenomenon in the ^{27}Al+^{27}Al system at lower incident energies (116–122) MeV. In this way it is shown that non-statistical fluctuations are present in the EF on a quite large incident energy range. In the present article more precise results concerning the DNS deformation, are reported. From the analysis of the EAF structure at $\varepsilon > 0$ in corroboration with the $\langle$TKE$\rangle$ value, a separation distance value from 10.0 to 10.9 fm has been obtained indicating a large deformation of the excited rotational states as in the case of the light non-α system ^{19}F+^{27}Al previously studied by us. If the deformation found on this basis for the ^{19}F+^{27}Al DNS was already evidenced in the corresponding CN (^{46}Ti) by experiments studying GDR and α particle spectra, the confirmation of the deformation for the ^{27}Al+^{27}Al DNS remains an aim of future experiments. The experimental evidence from the present article supports a reaction mechanism where special states of rotational (molecular) nature play the role of doorway configurations toward a regime characterized by stochastic exchange of nucleons between interacting nuclei as the main mechanism behind the dissipative phenomena in light heavy-ion collisions.

ACKNOWLEDGMENTS

For the high-quality targets we owe special acknowledgment to Mr. C. Marchetta. We acknowledge Professor E. Migneco and D. Vinciguerra for their support. We are grateful to the operating crew of LNS Tandem accelerator for the quality of the delivered beam.

[1] A. De Rosa, G. Inglima, V. Russo, M. Sandolini, G. Fortuna, G. Montagnoli, C. Signorini, A. M. Stefanini, G. Cardella, G. Pappalardo, and F. Rizzo, Phys. Lett. **B160**, 239 (1985).
[2] R. Bonetti and M. S. Hussein, Phys. Rev. Lett. **57**, 194 (1986).
[3] A. Y. Abul-Magd and M. H. Simbel, Phys. Lett. **B83**, 27 (1979).
[4] K. M. Hartmann, W. Dünweber, and W. E. Frahn, Nucl. Phys. **A380**, 170 (1982).
[5] A. Glaesner, W. Dünnweber, W. Hering, D. Konnerth, R. Ritzka, R. Singh, and W. Trombik, Phys. Lett. **B169**, 153 (1986).
[6] T. Suomijärvi, B. Berthier, R. Lucas, M. C. Mermaz, J. P. Coffin, G. Guillaume, B. Heusch, F. Jundt, and F. Rami, Phys. Rev. C **36**, 181 (1987).
[7] A. De Rosa, G. Inglima, M. Romano, V. Russo, M. Sandoli, G. Cardella, G. Pappalardo, F. Rizzo, G. Fortuna, A. M. Stefanini, S. Beghini, G. Montagnoli, and C. Signorini, Phys. Rev. C **37**, 1042 (1988).
[8] F. Rizzo, G. Cardella, A. De Rosa, A. Di Pietro, A. D'Onofrio, E. Fioretto, G. Inglima, M. Papa, G. Pappalardo, M. Romano, M. Romoli, F. Terrasi, M. Sandoli, and G. S. Wang, Z. Phys. A **349**, 169 (1994).
[9] G. Cardella, M. Papa, G. Pappalardo, F. Rizzo, Q. Wang, A. De Rosa, E. Fioretto, G. Inglima, M. Romoli, M. Sandoli, R. Setola, L. Corradi, G. Montagnoli, and A. M. Stefanini, Z. Phys. A **336**, 387 (1990).
[10] M. Papa, G. Cardella, A. Di Pietro, S. L. Li, A. Musumarra, G. Pappalardo, F. Rizzo, A. De Rosa, G. Inglima, M. La Comarra, D. Pierroutsakou, and M. Romoli, Z. Phys. A **353**, 205 (1995).
[11] Wang Qi, Lu Jun, Xu Hushan, Li Songlin, Zhu Yongtai, Fan Enjie, Yin Xu, Zhang Yuhu, Li Zhichang, Zhao Kui, Lu Xiuqin, and Hu Xiaoqing, Phys. Lett. **B388**, 462 (1996).
[12] M. Papa, Ph.D. thesis, VI Cycle, Catania University, 1994 (in Italian).
[13] M. Papa, F. Amorini, G. Cardella, M. Cavallaro, P. Figuera, A. Musumarra, G. Pappalardo, F. Rizzo, S. Romano, S. Tudisco, B. Heusch, Wang Qi, Si Songlin, Lu Jun, Tian Wendong, and Hu Pengyu, Phys. Rev. C **61**, 044614 (2000).
[14] C. Beck, R. Nouicer, D. Disdier, G. Duchêne, G. de France, R. M. Freeman, F. Haas, A. Hachem, D. Mahboub, V. Rauch, M. Rousseau, S. J. Sanders, and A. Szanto de Toledo, Phys. Rev. C **63**, 014607 (2001).
[15] M. Lattuada, D. Vinciguerra, C. M. Sutera, G. Inglima, and M. Sandoli, Phys. Rev. C **35**, 818 (1987).
[16] L. Vanucci, U. Abbondanno, M. Bettiolo, M. Bruno, N. Cindro, M. D'Agostino, P. M. Milazzo, R. A. Ricci, T. Ritz, W. Scheid, and G. Vannini, Z. Phys. A **355**, 41 (1996).

[17] I. Berceanu *et al*., Phys. Rev. C **57**, 2359 (1998).
[18] A. Pop, A. Andronic, I. Berceanu, M. Duma, M. Moisă, M. Petrovici, V. Simion, A. Bonasera, G. Immé, G.Lanzanò, A. Pagano, G. Raciti, N. Colonna, G. d'Erasmo, A. Pantaleo, H. Feldmeier, and J. Schnack Nucl. Phys. **A679**, 793 (2001).
[19] S. Yu. Kun, A. V. Vagov, and O. K. Vorov, Phys. Rev. C **59**, R1 (1999).
[20] S. Yu. Kun, B. A. Robson, and A. V. Vagov, Phys. Rev. Lett. **83**, 504 (1999).
[21] W. W. Wilcke, J. R. Birkelund, A. D. Hoover, J. R. Huizenga, W. U. Schröder, and H. J. Wollersheim, *Table of Reaction Parameters for Heavy-Ion Collisions*, At. Data Nucl. Data Tables **25**, 391 (1980).
[22] C. Beck and A. Szanto de Toledo, Phys. Rev. C **53**, 1989 (1996).
[23] A. Richter, in *Nuclear Spectroscopy and Reactions*, edited by J. Cerny (Academic Press, New York, 1974), Vol. B, p. 343.
[24] G. Pappalardo, Phys. Lett. **13**, 320 (1964).
[25] R. Singh, K. A. Eberhard, and R. G. Stokstad, Phys. Rev. C **22**, 1971 (1980).
[26] D. Shapira, R. G. Stokstad, and D. A. Bromley, Phys. Rev. C **10**, 1063 (1974).
[27] C. K. Gelbke, C. Olmer, M. Buenerd, D. H. Hendrie, J. Mahoney, M. C. Mermaz, and D. K. Scott, Phys. Rep. **42**, 311 (1978).
[28] A. Pop, A. Andronic, I. Berceanu, A. Buţă, M. Duma, M. Moisă, M. Petrovici, V. Simion, G. Immé, G. Lanzanò, A. Pagano, G. Raciti, R. Coniglione, A. Del Zoppo, P. Piatelli, P. Sapienza, N. Colonna, G. d'Erasmo, and A. Pantaleo, *Proceeding of the European Conference on Advances in Nuclear Physics and Related Areas, Thessaloniki, Greece, July 1997*, edited by D. M. Brink, M. E. Grypeos and S. E. Massen (Giahoudi-Giapouli Publishing, Thessaloniki, Greece, 1999), ISBN 960-7425-29-4, p. 653.
[29] T. Ericson, Ann. Phys. **23**, 390 (1963).
[30] D. M. Brink and K. Dietrich, Z. Phys. A **326**, 7 (1987).
[31] H. Breuer, N. R. Yoder, A. C. Mignerey, V. E. Viola, K. Kwiatkowsky, and K. L. Wolf, Nucl. Instrum. Methods **204**, 419 (1983).
[32] Yu. S. Kun, Phys. Lett. **B257**, 247 (1991).
[33] Yu. S. Kun, W. Nörenberg, and M. Papa, Phys. Lett. **B298**, 273 (1993).
[34] U. Abbondanno, Phys. Rev. C **43**, 1484 (1991).
[35] C. K. Gelbke, P. Braun-Munzinger, J. Barette, B. Zeidman, M. J. Levine, A. Gamp, H. L. Harney, and Th. Walcher, Nucl. Phys. **A269**, 460 (1976).
[36] J. B. Natowitz, M. N. Namboodiri, R. Eggers, P. Gonthier, K. Geofferoy, R. Hanus, C. Towsley, and K. Das, Nucl. Phys. **A277**, 477 (1977).
[37] G. Wolshin and W. Nörenberg, Z. Phys. A **284**, 209 (1978).
[38] M. Petrovici, A. Andronic, I. Berceanu, A. Buţă, M. Duma, D. Moisă, A. Pop, V. Simion, A. Bonasera, G. Immé, G. Lanzanò, A. Pagano, G. Raciti, N. Colonna, G. d'Erasmo, and A. Pantaleo, Z. Phys. A **354**, 11 (1996).
[39] C. Bhattacharya, M. Rousseau, C. Beck, V. Rauch, R. M. Freeman, D. Mahboub, R. Nouicer, P. Papka, O. Stezowski, A. Hachem, E. Martin, A. K. Dummer, S. J. Sanders, and A. Szanto De Toledo, Phys. Rev. C **65**, 014611 (2001).
[40] D. K. Agnihotri, A. Kumar, K. C. Jain, K. P. Singh, G. Singh, D. Kabiraj, D. K. Avasthi, and I. M. Govil, Phys. Lett. **B307**, 283 (1993).
[41] S. M. Lee, T. Matsuse, and A. Arima, Phys. Rev. Lett. **45**, 165 (1980).
[42] S. Yu. Kun, U. Abbondanno, M. Bruno, N. Cindro, M. D'Agostino, P. M. Milazzo, R. A. Ricci, T. Ritz, B. A. Robson, W. Scheid, A. V. Vagov, G. Vannini, and L. Vannucci, Z. Phys. A **359**, 145 (1997).
[43] S. Cohen, F. Plasil, and W. J. Swiatecki, Ann. Phys. **82**, 557-596 (1974).
[44] E. Uegaki and Y. Abe, Phys. Lett. **B340**, 143 (1994).
[45] R. Nouicer, C. Beck, R. M. Freeman, F. Haas, N. Aissaoui, T. Bellot, G. de France, D. Disdier, G. Duchêne, A. Elanique, A. Hachem, F. Hoellinger, D. Mahboub, V. Rauch, S. J. Sanders, A. Dummer, F. W. Prosser, A. Szanto De Toledo, Sl. Cavallaro, E. Uegaki, and Y. Abe, Phys. Rev. C **60**, 041303 (1999).
[46] C. Beck, R. Nouicer, D. Disdier, G. Duchêne, G. de France, R. M. Freeman, F. Haas, A. Hachem, D. Mahboub, V. Rauch, M. Rousseau, S. J. Sanders, and A. Szanto De Toledo, Phys. Rev. C **63**, 014607 (2000).
[47] D. Mahboub, C. Beck, B. Djerroud, R. M. Freeman, F. Haas, R. Nouicer, M. Rousseau, P. Papka, A. Sànchez i Zafra, Sl. Cavallaro, E. De Filippo, G. Lanzanò, A. Pagano, M. Sperduto, E. Berthoumieux, R. Dayras, R. Legrain, E. Pollacco, and A. Hachem, Phys. Rev. C **69**, 034616 (2004).
[48] A. Maj, M. Kmiecik, M. Brekiesz, J. Grebosz, W. Meczyński, J. Styczeń, M. Ziebliński, K. Zuber, A. Bracco, F. Camera, G. Benzoni, B. Million, N. Blasi, S. Brambilla, S. Leoni, M. Pignanelli, O. Wieland, B. Herskind, P. Bednarczyk, D. Curien, J. P. Vivien, E. Farnea, G. De Angelis, D. R. Napoli, J. Nyberg, M. Kicińska-Habior, C. M. Petrache, J. Dudek, and K. Pomorski, Eur. Phys. J. A **20**, 165 (2004).
[49] A. Maj, M. Kmiecik, A. Bracco, F. Camera, P. Bednarczyk, B. Herskind, S. Brambilla, G. Benzoni, M. Brekiesz, D. Curien, G. De Angelis, E. Farnea, J. Grebosz, M. Kicińska-Habior, S. Leoni, W. Meczyński, B. Million, D. R. Napoli, J. Nyberg, C. M. Petrache, J. Styczeń, O. Wieland, M. Ziebliński, K. Zuber, N. Dubray, J. Dudek, and K. Pomorski, Nucl. Phys. **A731**, 319 (2004).
[50] M. Brekiesz, P. Papka, A. Maj, M. Kmiecik, C. Beck, P. Bednarczyk, J. Grebosz, F. Haas, W. Meczyński, V. Rauch, M. Rousseau, A. Sànchez i Zafra, J. Styczeń, S. Thummerer, M. Ziebliński, and K. Zuber, Acta Phys. Pol. B **36**, 1175 (2005).
[51] P. Papka, C. Beck, F. Haas, V. Rauch, M. Rousseau, P. Bednarczyk, S. Courtin, O. Dorvaux, K. Eddahbi, J. Robin, A. Sànchez i Zafra, O. Stezowski, and A. Prévost, Acta Phys. Pol. B **34**, 2343 (2003).